RASĀYAN *J. Chem.*
Vol. 17 | No. 4 |1957-1966| October - December | 2024
ISSN: 0974-1496 | e-ISSN: 0976-0083 | CODEN: RJCABP
http://www.rasayanjournal.com
http://www.rasayanjournal.co.in

ENHANCING ANTICORROSIVE PROPERTY OF MILD STEEL COATED BY SYNTHESIZED EUGENOL-BASED BENZOXAZINE WITH 3-ACETYL PHENYL SIDE CHAIN AND COPOLYMERIZING WITH URETHANE

S. Elavarasan[1,✉], N. Vijayakumari[2] and D. Anbuselvi[3]
[1]Department of Chemistry, Muthayammal Engineering College (Autonomous) Namakkal, India
[2]Department of Chemistry, Government Arts College for Women, Salem, India
[3] Department of Physics, T. John Institute of Technology, Bangalore, India
✉Corresponding author: prince2chem@gmail.com

ABSTRACT
The reaction of paraformaldehyde, 3-amino acetophenone, and eugenol yields EuBz-based Benzoxazine monomer (EuBz-ap), which is then characterized by FT-IR,1H NMR, and UV-visible spectroscopic techniques. The produced monomer is then cured by applying it to mild steel (MS) using a polyurethane (PU) hardener. Furthermore, investigations using electrochemical polarization examine the impact of varying PU hardener concentrations on mild steel coated with EuBz-ap-PU and combined with benzoxazine monomer on gel and water absorption. The findings show that the coating's anticorrosive qualities are improved with increased PU concentrations. Moreover, Density Functional Theory (DFT) computations are employed to validate the corrosion resistance of the material.
Keywords: Mild steel, Eugenol, Polybenzoxazine, DFT, Polarization, Corrosion Protection, Dip- Coatings
RASĀYAN*J. Chem.*, Vol. 17, No. 4, 2024

INTRODUCTION

Metals are used in a lot of different fields, like construction, transportation, and medicine. To endure longer, the metal layer should be protected, which is often finished with paint. Coatings, on the other hand, can be used for a variety of things to protect against corrosion, fogging, icing, biofilm adhesion, and other potential losses in value.[1]One of the significant issues that outcomes in endless monetary and natural misfortunes consistently is erosion. As per one definition, it is the breakdown and debasement of materials achieved by the collaboration of such materials with their encompassing environments.[2] It hurts the construction, transportation, chemical, and manufacturing industries.[2]To address corrosion issues, numerous methods have been extensively utilized and researched. One of the most famous ways of forestalling erosion is to apply natural coatings, which enormously increment the help life of metallic substrates and save costs. However, for use in extremely hostile environments, ordinary organic coatings frequently lack the necessary anti-corrosion effectiveness. Coatings made of polymers are a viable option for dealing with these problems. Polymer coatings offer an unmistakable guard against destructive specialists. To safeguard the metal substrate from decay, these actual hindrances get it far from destructive particles, water, and oxygen. Consolidating blocker-stacked compartments, for example, multi-facet twofold hydroxides, halloysite nanotubes, and mesoporous SiO_2 nanocontainers, into coatings empowers the combination of dynamic consumption security, usually known as self-mending, accordingly improving enemy of erosion viability.[3,6]In addition, eco-friendly nanofillers that promote anti-corrosion properties or follow guidelines for corrosion inhibition can mitigate and prevent the onset of corrosion.[7]Among the myriad of polymer coatings, polybenzoxazine stands out as a thermosetting resin exhibiting significant potential, particularly in advanced coating applications.[8]Because benzoxazines have a complicated molecular structure and there are many different phenolic and amino derivatives accessible, researchers can create polymers with remarkable molecular structural flexibility.[9] This versatility makes PBZ an attractive option for various fields, including advanced coatings. For instance, applying a relieved polybenzoxazine (PBA-ddm) covering to mild steel forestalled basic erosion and diminished the pace of consumption by two significant degrees when contrasted with the untreated MS.[7]A few undertakings

involved polybenzoxazine coatings for electrical, heat-proof, and extremely hydrophobic surfaces at higher temperatures. To expand the utilization of polybenzoxazine, silane-functionalized polybenzoxazine was likewise utilized as an anti-corrosion covering on steel surfaces. This defensive covering was explicitly intended to limit the pace of erosion on steel, with the viability of diminishing the consumption current multiple times that of an unadulterated MS surface.[10,11]Several researchers have explored a wide array of inhibition strategies, ranging from organic and inorganic compounds to nanoparticles, plant extracts, and polymers.[11-15] These inhibitors have been sought after because of their accessibility, intrinsic stability, low cost, and cost-effectiveness, making them attractive options for corrosion prevention in various industries. It is significant to safeguard these metals and metal compounds from this obliteration. As of late, among the polymers, polybenzoxazine, which is prestigious for its adaptability in the sub-atomic plan, framed a thermosetting polymer during the relieving system without the requirement for an impetus, and due to its high warm soundness and low hydrophobicity esteem, it assumes a critical part in the concealment of consumption. Thus, we accept that making the benzoxazine monomer more hydrophobic could keep water from sticking to it. Benzoxazine polymers can turn out to be less fragile when joined with polyurethanes, while polyurethanes can turn out to be more thermo-stable when joined with benzoxazine. At last, we choose to concentrate on creating a unique co-polymer that is harder, has less water absorption, and is thermally stable. As a result, we have created a co-polymer of benzoxazine and polyurethane that is more hydrophobic and acts as a barrier against harmful substances. To analyze the elements of erosion hindrance, three unique Bz: Ratios of PU were developed. Besides, a thorough examination of the electronic way of behaving of the monomer was done using DFT examination and sub-atomic natural planning; the results show the sub-atomic electronic state of the monomer's surface. Potentiometry and electrochemical analysis were applied to each of the three co-polymers, and the results are fully presented.[20,21]

EXPERIMENTAL

Common Approaches

The IR spectra were documented utilizing a Thermo Logical Nicolet iS50 FT-IR Spectrometer, while UV spectra were gotten with a Labman LMSP UV-1200 UV-Vis spectrometer. To affirm the consummation of the response through the standard convention, tender loving care was performed, and 1H NMR was directed on a Bruker 500MHz instrument involving DMSO-D6 as the dissolvable. Ag/AgCl filling in as the reference terminal and Pt serving as the counter anode was used in polarization tests performed utilizing the Biologic SP 300 model, a 3-cathode cell framework. Water retention tests for restored covering tests were executed as per ASTM D570 guidelines. The recovered testing underwent a 24-hour room temperature immersion in water after being dried at 80ºC in a vacuum burner. Consequently, the specimens were extracted from the water, blotched using tissue paper, and weighed in order to determine the water retention rate. Weighing was used to determine the coated, cured samples' total gel content. After being soaked for 24 hours at room temperature, covered plates were weighed when they were removed from the xylene. After the coated samples had been dried in a vacuum oven, their gel content was evaluated. Computational estimations, including the portrayal of the Greatest Involved Sub-atomic Orbital (HOMO) and Least Abandoned Atomic Orbital (LUMO) in the designated spot records, were performed utilizing the Gaussian 09W program utilizing thickness useful hypothesis with the B3LYP/6.31 G premise set. Perception of processed structures, incorporating HOMO, LUMO, and Sub-atomic Electrostatic Potential (MEP) portrayals, was worked with utilizing the GaussView programming bundle.

Synthesis of EuBz-ap Monomer (1-(3-(6-allyl-8-methoxy-2H-benzo[e][1,3]oxazin-3(4H)-yl)phenyl)ethan-1-one)

In 20mL of chloroform, the paraformaldehyde (0.34g) and 3-amino acetophenone were dissolved and it was stirred for 30 minutes at 50°C to synthesize the EuBz-ap monomer. After that, eugenol (1g) and additional chloroform (80 mL) were mixed, and the assortment was refluxed for sixteen hours at 80°C. Employing TLC, the reaction's progress was observed. Following the completion of the reaction, 150 mL of chloroform was added to the mixture, and it was then cleaned using 200mL of 1N NaOH solution, 100mL of water, and 100mL of NaCl solution. After separating the organic layer and drying it with anhydrous sodium sulfate, the EuBz-ap monomer was extracted.

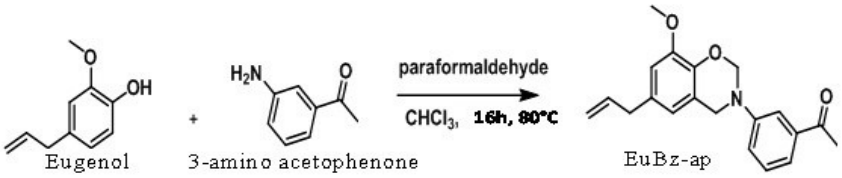

Synthesis of EuBz-ap-PU Copolymers

EuBz-ap (400 mg) was broken up in 1,4-dioxane (1 mL) and joined with fluctuating proportions of polyurethane hardener in toluene (1 mL), bringing about three various compositions of EuBz-ap monomer and polyurethane blends (100:60, 100:80, &100:100). Gentle mild steel plates were fastidiously cleaned utilizing water, ethanol, hexane, and" CH3)2CO. In order to improve attachment, abrasive paper of different grades was used to polish the steel surface. The method was carried out ten times: the gently arranged mild steel was submerged in the EuBz-ap: PU solution for one minute, and then it was gradually taken out of the solution. Following that, the coated mild steel was maintained in a hot air oven at 100°C for one hour and thermally cured for two hours in a furnace at 200°C. The coated mild steel was further studied through polarization and surface analysis.

RESULTS AND DISCUSSION

NMR Spectrum of the EuBz-ap Monomer

Using a nuclear magnetic resonance spectrophotometer, the EuBz-ap monomer's structure was examined and found to be true. 1H was used to approve the monomer structure. Methoxy protons, which upon integration appear as three protons in Figure -1, are the tops at 3.3 ppm. The presence of four protons and one proton, separately, in the benzoxazine ring is shown bythe tops seen at 5.0 and 2.5 ppm, which uphold the blend of benzoxazine.

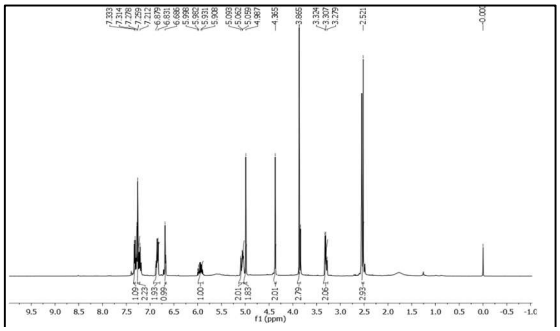

Fig.-1: ^{1}H NMR Spectrum of Monomer EuBZ-ap

IR Spectrum of Pure EuBz-ap and EuBz-ap blends with PU

Figure-2 shows the analysis of the FT-IR spectra of the monomer and each copolymer that contained the monomer and isocyanate hardener. The -CH bonds from the $-CH_2$ groups of the benzoxazine and eugenol side chains were found to be stretched symmetrically at wave numbers 2946cm^{-1} and asymmetrically at 2857cm^{-1}, respectively. In addition, the -C-O-asymmetric stretching frequency was indicated by a band at 1279cm^{-1}, whereas the symmetric stretching of the identical bond was represented by a band at 1227cm^{-1}. A band that appeared at 925cm^{-1} suggested that a benzoxazine ring was present. The polyurethane linked to the polybenzoxazine exhibits a -N-H stretching frequency, which was indicated by a band at 3450cm^{-1}. Meanwhile, another aromatic -CH band was observed at 1504cm^{-1}. Additionally, the benzoxazine monomer's carbonyl group showed a peak at 1673cm^{-1}.

UV-Vis Studies of Pure EuBz-ap and EuBz-ap blends with PU

The UV-Vis range was recorded utilizing a Labman LMSP UV-1200 UV-Vis spectrometer. Electronic spectroscopy, usually alluded to as UV-noticeable spectroscopy, is utilized to analyze the electronic

change of natural mixtures. There are two absorption bands at 278,282,284 and 293 nm in the monomer and monomer with a combination of PU UV-visible spectra, respectively. The absorbance appears as a result of the monomer's π-π* and n-π* transitions alone or when combined with PU.

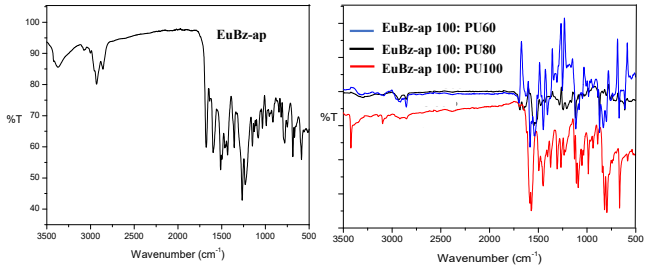

Fig.-2: (a) and (b) FT-IR spectrum of EuBz-ap and EuBz-ap blends with PU

Both the monomer and the monomer related to PU had absorbances of 278,282,284 and 293 nm, separately. Figure-3 shows the UV-apparent spectra at 278,282,284 and 293 nm, separately. In addition, the absorbance was increased by the band associated with the n-π* transition, indicating that polyurethane significantly induced the electronic transition of the monomer. Given this, it is reasonable to anticipate that synthesized copolymers will have improved corrosion resistance.[15,16]

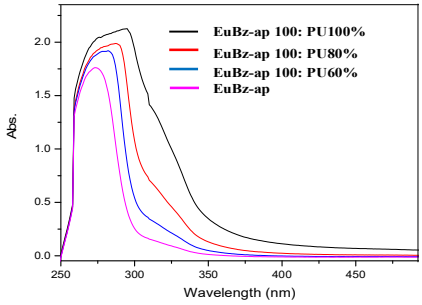

Fig.-3:UV-Visible spectrum of EuBz-ap and EuBz-ap blends with PU

Mass Spectrum of Pure EuBz-ap Monomer

One common analytical approach for evaluating an ion's mass-to-charge ratio is mass spectrometry . A mass spectrum, a graphical depiction of intensity as a function of mass-to-charge ratio, is commonly utilized to display the results. MS finds application across diverse fields, where it is utilized not only for the analysis of pure samples but also for the examination of complex mixtures. The synthesized compound is at last affirmed by mass spectroscopy. For that, the particle is melted in the methanol and examined at 1 µM fixation. For the compound, the M+1 top is found as a sub-atomic particle top which is the parent particle top in the range hence approving the compound's development. The sub-atomic particle top saw at 324.12 for $[M+1]^+$for the atom in the positive method of range. Figure-4 depicts the monomer's mass spectrum.

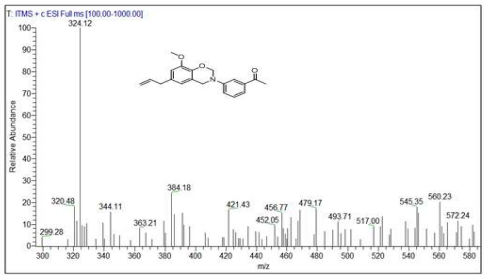

Fig.-4: Mass spectrum of pure EuBz-ap Monomer

Potentiostatic Polarization Estimations

Polarization estimations were led utilizing a traditional three-cathode cell arrangement. Mild steel strips coated with EuBz-ap and PU hardener in varying concentrations (EuBz: PU, 100:60, 100:80, & 100:100) as the working electrode, were used exclusively on an exposed area of one-centimeter square. The Tafel extrapolation method was used to assess the coatings' resistance to corrosion. Tafel polarization bends produced from the examples are portrayed in Figure -5.These curves were used to calculate "the corrosion potential (Ecorr) and corrosion current (Icorr). By superimposing a straight line along the direct section of the cathodic or anodic bend and extrapolating it across the erosion potential, the consumption current is not completely fixed. An Ecorr that is more negative and has a larger Icorr typically indicates a faster rate of corrosion; whereas an Ecorr that is less negative and has a smaller Icorr indicates a process that is more gradual.[17] The following formulas were employed to calculate the corrosion rate as well as corrosion efficiency.[18]

Corrosion rate = $(Icorr \times K \times EW)/\rho A$ mmpy

Where, K=3272mmyear^{-1} (rate constant), the equivalent weight of the mild steel (EW) (27.9g), the mild steel density (ρ=7.85gcm^{-3}), and the area of the sample (A=1cm^2).

Corrosion efficiency (%) = $[(Icorr(b)-Icorr(c))/(Icorr(b))] \times 100$

Where, Icorr(b) is the corrosion current for the uncoated MS plate, Icorr(c) is the corrosion current for the EuBz-ap-PU coated" MS plates.

Ecorr is the corrosion potential, and the addition of polyurethane hardener to the coating indicates this. This observation suggests that the EuBz-ap-PU coating provides superior corrosion protection to the benzoxazine coating on the MS surface. The stretching and cross-linking densities of the polymeric materials usually have an impact on the rate of water permeability through polymeric films. The cross-linking density rises in conjunction with the coating's polyurethane concentration. Thus, the elevated cross-connecting thickness of the EuBz-ap-PU covering lessens porosity and strengthens consumption obstruction properties. The resultant erosion opposition properties are additionally supported by low consumption rates and higher erosion productivity of up to, not entirely set in stone from electrochemical estimations.

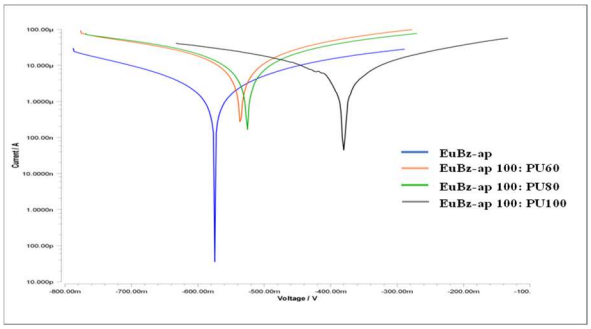

Fig.5 Tafel polarization curves for the EuBz-ap and EuBz-ap-PU on mild steel

Table-1: Electrochemical behavior of EuBz-ap and EuBz-ap-PU on mild steel in 3.5% NaCl

Scanning Electron Microscopy Analysis

Using scanning electron microscopy (SEM) analysis, the surface morphology of the mild steel was examined after it had been submerged in 3.5 percent NaCl for seven days. The acquired information exhibits that both before (Figures.-6a, b, and c), and after immersing the coated mild steel for a week in 3.5% NaCl Fig.-6b and c, then again, show that gentle steel covered in the proportions of 100:80 and 100:100 with EuBZ-ap-PU has not eroded so much. This is because the mild steel's surface has developed a protective layer due to the isocyanate oxygen atom's ability to cross-link after immersion in NaCl. Accordingly, Urethane polymer along with eugenol-based benzoxazine safeguards the gentle steel in a 3.5% NaCl climate.

Fig.-6(a): EuBz-ap - PU(100:60) Before and After immersion in 3.5% NaCl

Fig.-6(b): EuBz-ap-PU(100:80) Before and After immersion in 3.5% NaCl

Fig.-6(c): EuBz-ap-PU(100:100) Before and After immersion in 3.5% NaCl

Microscopic Analysis

As with any study of corrosion, the environment of interest must be chosen carefully. The selection of the water chemistry for a nuclear reactor is based on maximizing the thermal performance and maximizing the lifetime of the components (by reducing environmental degradation and the release of corrosion products). Other than its monetary effect, erosion influences well-being, security, and the climate. Consumption influences all ventures, like oil and gas and asset areas, and most parts of human exercises. The images of the image before and after loading monomer in this result (Figure -7): 60, 80, and 100 PU in 3.5% NaCl-created polymeric materials has really relieved erosion. By increasing the amount of polyurethane, the corrosion has been markedly reduced, which is noteworthy. For instance, tests 100-60 display a cleaned surface rather than the untreated example after consumption, with additional improvement seen in the example covered with 80% polyurethane (100-80). Additionally, the example covered with 100 percent polyurethane shows almost no harshness on the gentle steel surface, likened to its pre-consumption state.

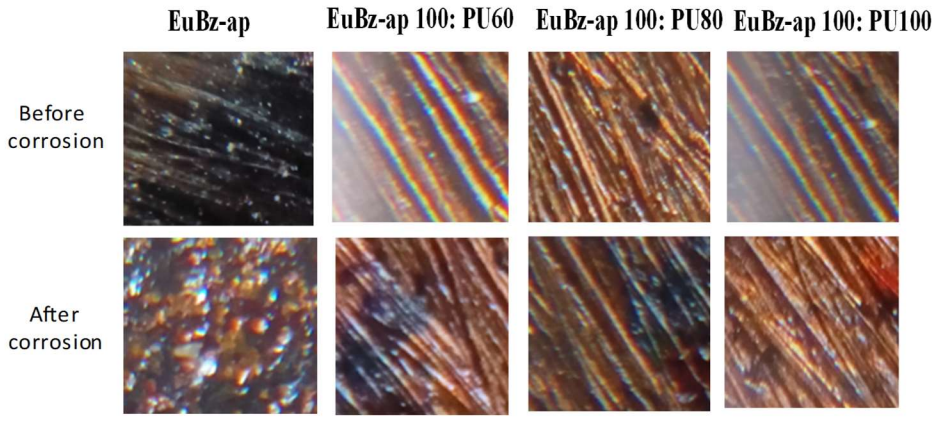

Fig.-7: Microscopic image of EuBz-ap-PU copolymer before and after immersion in 3.5% NaCl

Table-1

Concentration of samples (EuBz-ap:PU)	Tafel studies						
	Icorr (uA)	Ecorr (mV)	Tafel constant mv/decade		Corrosion Efficiency (%)	Surface Coverage (θ)	Corrosion Rate (mmpy)
			b_a	b_c			
100:0	7.280	-638	-179	159	-	-	84660.18
100:60	2.000	-584	-207	171	72.52	0.7252	23258.29
100:80	0.237	-534	8.74	-15.1	96.74	0.9674	2756.10
100:100	0.119	-508	13.2	-23.1	98.36	0.9836	1383.86

Quantum Compound Computations

Frontier molecular orbital (FMO) examination in DFT examinations has given the understanding of the synthetic reactivity of the delivered monomer. The Gaussian 09W software package was used throughout the DFT analysis. Corresponding to this examination, the monomer's 3D construction was first streamlined utilizing 3D ChemDraw, which was then stuck into Gaussian programming and analyzed utilizing the B3LYP/6.311 G premise set. The Gauss View software can be used to display the achieved optimal structure. It can then be used for various logical cycles, such as deciding the electron thickness of the atom and working out the sub-atomic electrostatic potential. Simply said, HOMO refers to the highest involved atomic orbital and LUMO for the lowest unoccupied particle orbital. While adamantane shows no electron thickness by any stretch of the imagination, HOMO and LUMO were tracked down in a similar region of the atom in the ongoing examinations the benzoxazine ring. Thickness utilitarian hypothesis (DFT) examination is one of the various uses of numerical calculation that find utility in engineered science, response organizing, and bio-scientific uses. The ground state and invigorated state atomic orbitals that fundamentally impact each other are known as boondocks sub-atomic orbitals. The area of the electron cloud and the electrical design of the particle might be uncovered by these orbitals. The lowest unoccupied molecular orbital is the lowest empty atomic orbital, and the highest occupied molecular orbital is the highest involved sub-atomic orbital. The upsides of the quantum synthetic descriptors, like the substance potential, whole energy (ΔEgap), worldwide delicateness (σ), worldwide hardness (η), and electrophilicity file, are displayed in the table. Even though adamantane displays no electron thickness by any stretch of the imagination, in the flow exploration, HOMO and LUMO were found in a similar locale of the particle the benzoxazine ring (Figures-8a,b & c). This is on the grounds that low electron thickness is the after-effect of pi-electrons not being able to exist in the aliphatic ring. The ΔE worth of a polybenzoxazine in light of ethylene and a PU copolymer with a 3-acetyl phenyl side chain is 4.205 eV (Table-2).

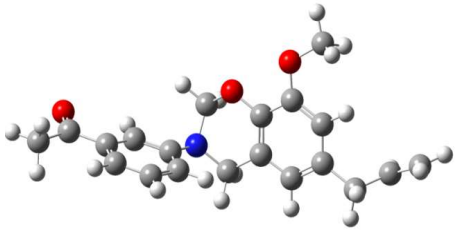

Fig.-8(a): Optimized structure of benzoxazine monomer (EuBz-ap)

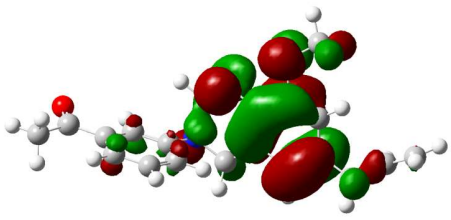

Fig.-8(b): Highest Occupied molecular orbital (EuBz-ap)

Table-2: DFT Parameters

S.No.	Highest occupied molecular orbital	Lowest unoccupied molecular orbital	Band gap	Chemical potential	Electrophilicity index
1	-5.4445	-1.2392	4.205	-3.3419	2.6557

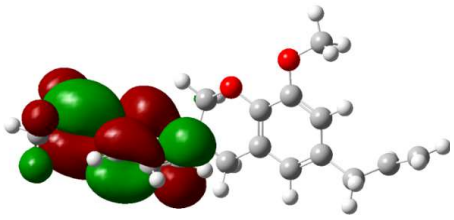

Fig.-8(c): Lowest unoccupied molecular orbital (EuBz-ap)

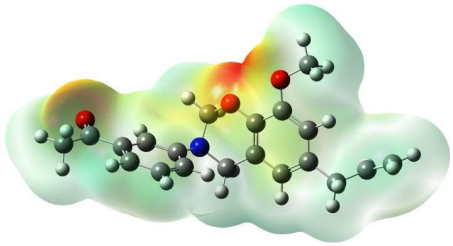

Fig.-8(d): Charge distribution of EuBz-ap monomer

Water Adsorption Studies

The hydrophobic idea of polymeric materials is a significant part of their improvement as hostile to steel consumption materials. The hydrophobic qualities of polymeric materials can be affected by their thickness of spreading and cross-connecting. The covering's folio movement additionally affected this property, bringing about the development of materials with bigger cross-thickness polymer contents and higher hydrogen holding limits. Polymers with higher urethane content are more likely to have lower water adsorption than their rivals because of this potential increase in hydrophobicity caused by urethane concentration. Figure-9 shows the water dispersion of monomers and every single polymeric complex. This remarkable result may be because of the phenyl ring, which makes the entire molecule more hydrophobic. This monomer alone (1.92%) has less water diffusion than previously observed. The extent of water dispersion falls as the polymeric material's urethane content increments, cresting at 0.79% for EuBZ-ap 100: PU 100. This study shows how the urethane and phenyl ring actual attributes enormously upgrade water dissemination limitations.The water absorption percentage was calculated by the following equation.[19]

$$\text{Percentage of water absorption} = [(W_a - W_b)/W_b] \text{ X } 100$$

Where,

Wa = Weight of the coated mild steel after removal of exposure to water absorption

Wb = Weight of the coated mild steel before removal of exposure to water absorption

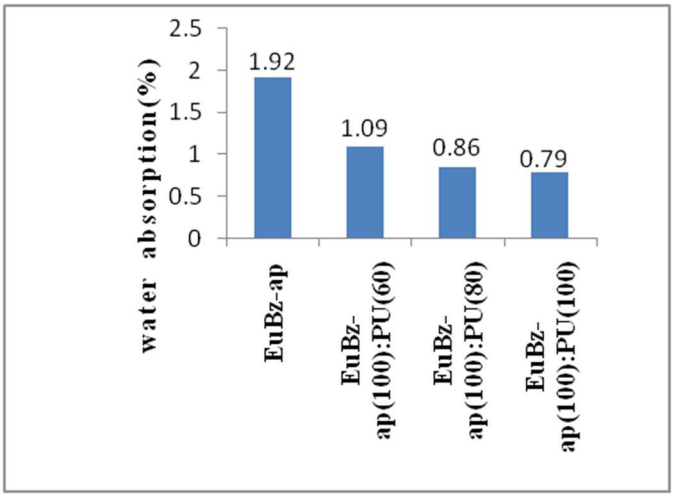

Fig.-9: Water absorption of EuBz-ap and EuBz-ap blends with PU

Gel Content Examinations

Gel development research is critical and may have a direct relationship with water dispersion research. Materials with more grounded intramolecular bonds can possibly diminish atomic porosity, which increments gel arrangement and diminishes water transport. From that point on, each polymeric and monomer material was explored; the results are displayed in Figure-10. The amount of urethane

significantly enhances the EuBZ-ap monomer's ability to form a gel, the 100 % urethane shows 90.11 % gel formation. The fact that all compounds, with the exception of monomers, gel more readily suggests that all polymeric materials should investigate their ability to resist corrosion. The following formula was used to determine the coating's gel content.[19]

$$\text{Percentage of gel content} = (W_a/W_b) \text{ X } 100$$

Where Wa and Wb are the weight of coated mild steel after and before the extraction respectively

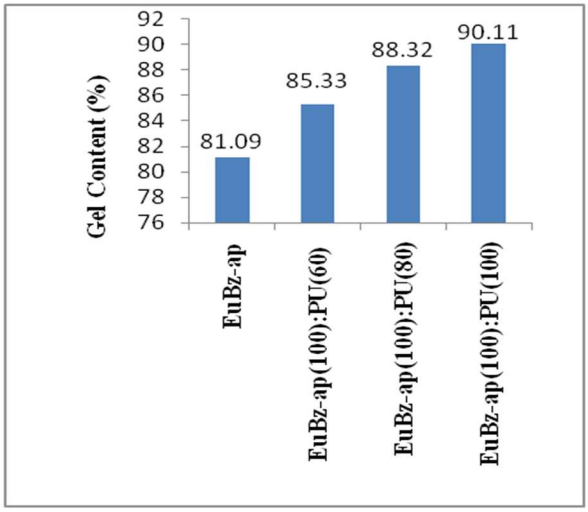

Fig.-10: Gel absorption of EuBz-ap and EuBz-ap blends with PU

CONCLUSION

In this review, we effectively orchestrate a monomer focused on benzoxazine utilizing an adamantane platform that is exceptionally hydrophobic. In addition, this is utilized in the creation of a corrosion-resistant co-polymer with polyurethane. A scope of centralizations of co-polymer including monomer and polyurethane was created and completely evaluated utilizing FT-IR, NMR, and UV-noticeable spectroscopy. In addition, a few physiographic characterizations were performed to gain additional insight into the copolymer capacity for water diffusion and gel formation. These discoveries propose that while concentrating on erosion, co-polymers are more helpful than monomers. Out of the three, 100 percent stacked polyurethane has the best co-polymer and has a dead sluggish erosion rate. This makes it a sublime enemy of destructive specialists with practically a 100 percent erosion restraint limit. The improvement of a synergistic effect between polyurethane and the hydrophobic monomer individuals may therefore be attributed to improved results. Additionally, SEM research demonstrates that materials with higher polyurethane content have superior mild steel anti-corrosive qualities.

ACKNOWLEDGMENTS

The creators might want to offer thanks to Dr. V. Raj, Professor and Head of the Department of Chemistry at Periyar University in Salem, India, for the consistent encouragement and suggestions that helped us finish this work.

CONFLICT OF INTERESTS

The creator announces no irreconcilable circumstance.

AUTHOR CONTRIBUTIONS

Every one of the creators contributed essentially to this original copy, partook in exploring/altering it, and approved the last draft for distribution. The authors' ORCID IDs can be used to confirm their research profile:

S. Elavarsan https://orcid.org/0009-0000-8251-773X
N. Vijayakumari https://orcid.org/0009-005-3193-0387
D. Anbuselvi https://orcid.org/0000-0002-6717-9821

REFERENCE

1. Yajun Deng, Lixue Xia, Guang-Ling Song, Yan Zhao, Yanmei Zhang, Yuqing Xu, and Dajiang Zheng, *Composites Part B: Engineering,* **225**, 109263, (2021), https://doi.org/10.1016/j.compositesb.2021.109263
2. Yitong Zhang, Xiaoyun Liu, Guozhu Zhan, Qixin Zhuang, Ruhong Zhang, and Jun Qian, *European Polymer Journal,* **119**,477(2019), https://doi.org/10.1016/j.eurpolymj.2019.07.020
3. E. Abdullayev, R. Price, D. Shchukin and Yuri Lvov, *ACS Applied Materials & Interfaces*, **1(7)**, 1437(2009), https://doi.org/10.1021/am9002028
4. Khairina Azmi Zahidah, Saeid Kakooei, Mokhtar Che Ismail, and Pandian Bothi Raja., *Progress in Organic Coatings,* **111**, 175(2017), https://doi.org/10.1016/j.porgcoat.2017.05.018
5. Elena Shchukina, Dmitry Grigoriev, Tatyana Sviridova, and Dmitry Shchukin, *Progress in Organic Coatings,* **108**, 84(2017), https://doi.org/10.1016/j.porgcoat.2017.03.018
6. Nedal Y. Abu-Thabit, and Abdel Salam Hamdy, *Surface and Coatings Technology,* **303**, 406(2016), https://doi.org/10.1016/j.surfcoat.2015.11.020
7. Ahmed M. M. Soliman, Kamal I. Aly, Mohamed Gamal Mohamed, Amer A. Amer, Mostafa R. Belal, and Mohamed Abdel-Hakim, *Scientific Reports,* **13(1)**, 5581(2023), https://doi.org/10.1038/s41598-023-30364-x
8. P. Thirukumaran, A. Shakila, and SarojadeviMuthusamy, *Rsc Advances,* **4(16)**, 7959(2014), https://doi.org/10.1039/C3RA46582A
9. Kan Zhang, Mengchao Han, Yuqi Liu, and Pablo Froimowicz, *ACS Sustainable Chemistry and Engineering,* **7(10)**, 9399(2019), https://doi.org/10.1021/acssuschemeng.9b00603
10. Changlu Zhou, Xin Lu, Zhong Xin, and Juan Liu., *Corrosion Science,* **70**, 145(2013), https://doi.org/10.1016/j.corsci.2013.01.023
11. Litong Wang, Manlin Yuan, Yudi Zhao, Zhen Guo, Xin Lu, and Zhong Xin, *Progress in Organic Coatings,* **167**, 106863(2022), https://doi.org/10.1016/j.porgcoat.2022.106863
12. S. C. Ikpeseni, H. I. Owamah, K. Owebor, E. S. Ameh, S. O. Sada, and E. Otuaro, *Journal of Bio and Tribo Corrosion,* **7(3)**, 84(2021), https://doi.org/10.1007/s40735-021-00505-8
13. D. De la Fuente, I. Díaz, J. Simancas, B. Chico, and M. J. C. S. Morcillo ,*Corrosion Science,* **53(2)**,604(2011), https://doi.org/10.1016/j.corsci.2010.10.007
14. M. J. Bahrami, S. M. A. Hosseini, and P. Pilvar, *Corrosion Science,* **52(9)**, 2793(2010), https://doi.org/10.1016/j.corsci.2010.04.024
15. Mary Stephanie S. Carranza, Yves Ira A. Reyes, Erick Christofer Gonzales, Danielle P. Arcon, and Francisco C. Franco, *Heliyon,* **7(9)**, e07952(2021), https://doi.org/10.1016/j.heliyon.2021.e07952
16. Sudha and Sarojadevi, *High Performance Polymers*, **28(3)**, 331(2016), https://doi.org/10.1177/0954008315580822
17. C. Zhou, X. Lu, Z. Xin, Y. Zhang, *Journal of Coating Technology and Research*, **13**, 63(2016) https://doi.org/10.1007/s11998-015-9722-z
18. K. Jayanthi1and M. Sivaraju, *Rasayan Journal of Chemistry,***16(2)**, 892904(2023), http://doi.org/10.31788/RJC.2023.1628362
19. K. Jayanthi1, M. Sivaraju and P. Shanmugasundaram, *Asian Journal of Chemistry,* **35(4)**, 851(2023), https://doi.org/10.14233/ajchem.2023.27290
20. Aeshah H. Alamri, Kedila Rasheeda, Salwa J. Kamal, Marwah Aljohani, Talal A. Aljohani, Irshad Baig, Vijaya DP Alva, N. Phadke Swathi, Ikenna B. Onyeachu, and SeranthimataSamshuddin, *Arabian Journal of Chemistry,* **17(6)**, 105752(2024), https://doi.org/10.1016/j.arabjc.2024.105752
21. Jayanthi Kannaiyan and Sivaraju Mani. *Oriental Journal of Chemistry,* **39(5)**, 1194(2023), http://dx.doi.org/10.13005/ojc/390512

[RJC- 8945/2024]